Indene Formation from Alkylated Aromatics: Kinetics and Products of the Fulvenallene + Acetylene Reaction

Gabriel da Silva*,† and Joseph W. Bozzelli*,‡

Department of Chemical and Biomolecular Engineering, The University of Melbourne, Victoria 3010, Australia, and Department of Chemistry and Environmental Science, New Jersey Institute of Technology, Newark, New Jersey 07102

Received: May 7, 2009; Revised Manuscript Received: June 23, 2009

A novel reaction is described for formation of the polyaromatic hydrocarbon (PAH) indene in aromatic flames, via the reaction of fulvenallene with acetylene (C_2H_2). Fulvenallene has been recently identified as the major decomposition product of the benzyl radical, the dominant intermediate in the oxidation of alkylated aromatic hydrocarbons, yet it is not presently included in kinetic models for aromatic oxidation or PAH/soot formation. Ab initio calculations with the G3B3 theoretical method show that acetylene adds to fulvenallene with a barrier of around 27 kcal mol^{-1}. This forms an activated C_9H_8 adduct that can rearrange to indene and dissociate to 1-indenyl + H with energy barriers below that of the entrance channel. Master equation simulations across a range of temperature and pressure conditions demonstrate that for temperatures relevant to combustion indene is the dominant product at high pressures while 1-indenyl + H dominate at lower pressures. At low to moderate temperatures, the production of collision stabilized cyclopentadiene-fulvene intermediates is also significant. The results presented in this study provide a new pathway to cyclopenta-fused PAHs in aromatic combustion and are expected to improve modeling of PAH and soot formation. The formation of cyclopenta-fused C_5-C_6 structures is required to describe the flame synthesis of carbon nanoparticles like fullerenes and buckybowls (corannulene). Improved rate expressions are also reported for the 1-indenyl + H → indene association reaction, and for the reverse dissociation, from variational transition state theory calculations. The new rate constants are significantly different than current estimates, primarily due to a re-evaluation of the indene C−H bond dissociation energy.

Introduction

The formation and growth of polyaromatic hydrocarbons (PAHs) in sooting flames is one of the most important yet least well understood problems in combustion chemistry (Scheme 1 illustrates several aromatics relevant to the present study). PAHs are a significant environmental and health concern, due to their role in soot formation,[1] and because of the carcinogenic and mutagenic properties of many PAHs.[2] The association of toxic PAHs with aerosols and ultrafine particulate matter[3] has been proposed to explain some of the negative health impacts of air pollution.[4] The chemistry of PAH formation is also relevant to the flame synthesis of carbon nanoparticles like fullerenes.[5] Fullerenes contain fused C_5-C_6 structures, known as cyclopenta-fused polyaromatic hydrocarbons (CP-PAHs); formation of the parent CP-PAH indene is a critical step in the production of carbon nanoparticles in sooting flames. Here, indene can grow to structures like corannulene ($C_{20}H_{10}$) via mechanisms including the addition of resonance stabilized radicals and hydrogen-abstraction/acetylene-addition (HACA).[6−8] Indene formation in sooting flames is described relatively poorly by existing kinetic models.[5,9,10]

The benzyl radical is a resonantly stabilized radical formed from aromatic precursors like toluene, and is a key species in the combustion of most commercial fuels and in PAH formation. Benzyl is thought to participate in PAH formation by reacting with acetylene (C_2H_2) to form indene + H,[11−13] by undergoing self-reaction to stilbene + 2H, and also by decomposing to a variety of PAH precursor molecules. The benzyl radical is rapidly oxidized by oxygen radical species like HO, HO_2, O,[14] and peroxy radicals, although it is relatively unreactive toward O_2.[15] Benzyl decomposes unimolecularly with a barrier of 80 to 90 kcal mol^{-1}, and temperatures of around 1500 K are required to effect pyrolysis.[16] Early studies on benzyl decomposition assumed that its decomposition products were the cyclopentadienyl radical (C_5H_5) + C_2H_2 and the propargyl radical (C_3H_3) + $2C_2H_2$ (or a C_4H_4 product). The further reactions of these decomposition products are used to explain sooting in toluene flames. It has now been demonstrated, both experimentally[17] and theoretically,[18,19] that the major products of benzyl decomposition are a C_7H_6 fragment + H.

Recent computational studies have revealed that fulvenallene is the previously unidentified C_7H_6 species in benzyl decomposition.[18,19] Fulvenallene is formed from benzyl with a barrier of around 85 kcal mol^{-1}, which is significantly lower than previously suggested pathways to $C_5H_5 + C_2H_2$.[20] Fulvenallene is the most stable isomer on the C_7H_6 potential energy surface[21] and has been detected at high levels in a toluene flame using photoionization mass spectrometry.[22] Furthermore, significant levels of a C_7H_6 species thought to be fulvenallene have been detected in a cyclopentene flame,[23] possibly due to the $C_5H_5 + C_2H_2$ reaction. Despite this, fulvenallene is absent from kinetic models for aromatic oxidation and PAH formation. This paper represents our first efforts to extend kinetic models of aromatic combustion to include the further reactions of fulvenallene. Here,

* To whom correspondence should be addressed. E-mail: (J.W.B.) bozzelli@njit.edu; (G.d.S.) gdasilva@unimelb.edu.au.
† The University of Melbourne.
‡ New Jersey Institute of Technology.

10.1021/jp904261e CCC: $40.75
Published on Web 07/15/2009

SCHEME 1: Polyaromatic Hydrocarbons (PAHs) and PAH Pre-Cursor Molecules of Relevance to the Present Study

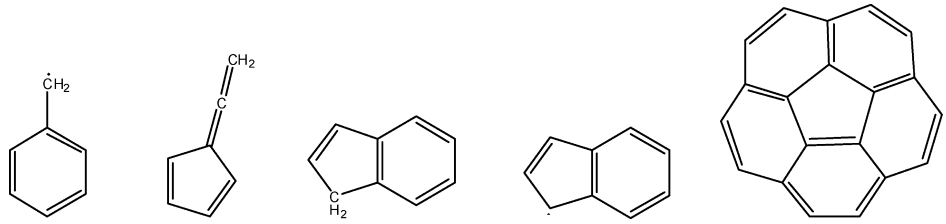

we identify a reaction between fulvenallene and acetylene that leads to the formation of indene (or the 1-indenyl radical plus H). High-level G3B3 quantum chemistry calculations and statistical reaction rate theory are used to model the fulvenallene + acetylene reaction kinetics, providing rate constants to the different product channels as a function of temperature and pressure.

Methods

Minima on the C_9H_8 potential energy surface are studied with the composite G3B3 theoretical method.[24] The G3B3 method uses B3LYP/6-31G(d) level optimized molecular geometries and vibrational frequencies with a series of higher-level corrections for accurate molecular energies. The G3B3 method reproduces the accurate experimental energies of the G2/97 test set with a mean error of 1 kcal mol^{-1},[24] and we propose that the enthalpies of reaction and activation reported here are accurate to ±2 kcal mol^{-1} (2σ).

Standard heats of formation ($\Delta_f H°_{298}$) are calculated for all species from G3B3 atomization enthalpies. Temperature-dependent thermochemical properties are evaluated from statistical mechanical principles. Corrections are applied for molecular symmetry and optical isomers where appropriate. Geometries, energies, and thermochemical properties ($S°_{298}$, $C_p(T)$) are available as Supporting Information. The Gaussian 03 program was used for all quantum chemistry calculations.[25]

High-pressure limit rate constants (k_∞) are calculated for all elementary reactions from 300 to 2000 K according to transition state theory (TST). Rate constants for the barrierless C−H bond dissociation in indene are obtained using variational transition state theory (VTST) and are described below. Rate constants have been fit to the apparent rate parameters E_a, A', and n ($k = A'T^n \exp(-E_a/RT)$), which we report here. These rate constants are corrected for reaction degeneracy as appropriate. Quantum tunnelling through the potential energy surface for the hydrogen shift reactions is accounted for using Eckart theory,[26] as described previously.[18,27] All transition state theory rate constant calculations are performed in ChemRate 1.5.2.[28]

Apparent rate parameters in the chemically activated fulvenallene + C_2H_2 mechanism are determined using quantum Rice−Ramsperger−Kassel (qRRK) theory with master equation (ME) treatment of falloff.[29] An exponential-down model is used for collisional energy transfer with $\langle\Delta E_{down}\rangle = 500$ cm^{-1}. Nitrogen (N_2) is used as the bath gas. The qRRK methodology accurately reproduces the results of full RRKM theory[18,29,30] using a reduced set of vibrational frequencies to calculate densities of states,[31] and was chosen here for its increased efficiency in treating reaction systems that include a relatively large number of intermediate species.

Results and Discussion

Reaction Mechanism. The proposed fulvenallene (**1**) + C_2H_2 reaction mechanism is depicted in Scheme 2. Acetylene associates with fulvenallene to form an activated C_9H_8 species (**2**), which isomerizes to cyclopentadiene-fulvene (**3**). From here, a reaction mechanism analogous to the well characterized fulvene-benzene rearrangement[32] takes place, ultimately resulting in the formation of indene (**6**) (Scheme 1 illustrates two isomeric channels for the cyclopentadiene-fulvene to indene rearrangement). Homolytic C−H dissociation in the activated indene molecule to the resonantly stabilized 1-indenyl (**7**) radical + H is also considered. Using this mechanism, we aim to show that the fulvenallene + C_2H_2 reaction produces C_9 polycyclic compounds, like indene and the 1-indenyl radical, at a rate significant enough to make a contribution to PAH formation in certain combustion processes.

Thermochemistry. Standard heats of formation for all identified stationary points, including transition states, are listed in Table 1 (numbering of these species is defined in Scheme 2 and Figure 5). Entropies and heat capacities (300−3000 K) are available for each species in the Supporting Information. Relatively few experimental values are available to compare to our calculated heats of formation (the acetylene heat of formation is of course well known at 54.19 kcal mol^{-1},[33] compared to 54.6 kcal mol^{-1} from our calculations). The indene heat of formation has been determined as 39.08 kcal mol^{-1},[34] again in good agreement with our calculated value, 39.8 kcal mol^{-1}. Marinov reported a 1-indenyl heat of formation of 61.98 kcal mol^{-1},[9] using a C−H bond dissociation energy (BDE) of 75.0 kcal mol^{-1}.[35] Our calculated 1-indenyl heat of formation, 68.6 kcal mol^{-1}, is significantly higher and results in a BDE of 80.9 kcal mol^{-1}. The more recent study of Richter et al.[36] used density functional theory and isodesmic reactions to calculate the 1-indenyl heat of formation as 65.01 kcal mol^{-1}, yielding a BDE of 78 kcal mol^{-1}. This is in better agreement with our results, but a difference of close to 3 kcal mol^{-1} remains. This discrepancy in the thermochemistry will effect the kinetics for loss of this weak H atom in indene via both dissociation and abstraction pathways, and rate constants for these important abstraction reactions may require re-evaluation.

VTST Calculations. The 1-indenyl radical associates with a H atom at one of the two degenerate radical C_5 ring sites without a barrier. The kinetics of this reaction and the reverse dissociation are treated here using variational transition state theory (VTST). The general VTST procedure is that described by da Silva and Bozzelli,[37] and has been used elsewhere to obtain rate constants for a range of barrier-less reactions.[14e,18,38] Rate constants for the 1-indenyl + H association and the reverse dissociation should prove useful in wider PAH modeling efforts, as well as being important in our present study.

The minimum energy potential (MEP) for C−H bond dissociation in indene is depicted in Figure 1. The MEP has been calculated at the B3LYP/6-31G(d) level of theory and has been scaled by the G3B3 reaction enthalpy (80.9 kcal mol^{-1}, versus 83.4 kcal mol^{-1} from B3LYP 0 K energies). The bond dissociation reaction is loose with no formal transition state

SCHEME 2: Mechanism for Indene (6) and 1-Indenyl (7) + H Formation from Fulvenallene (1) + Acetylene

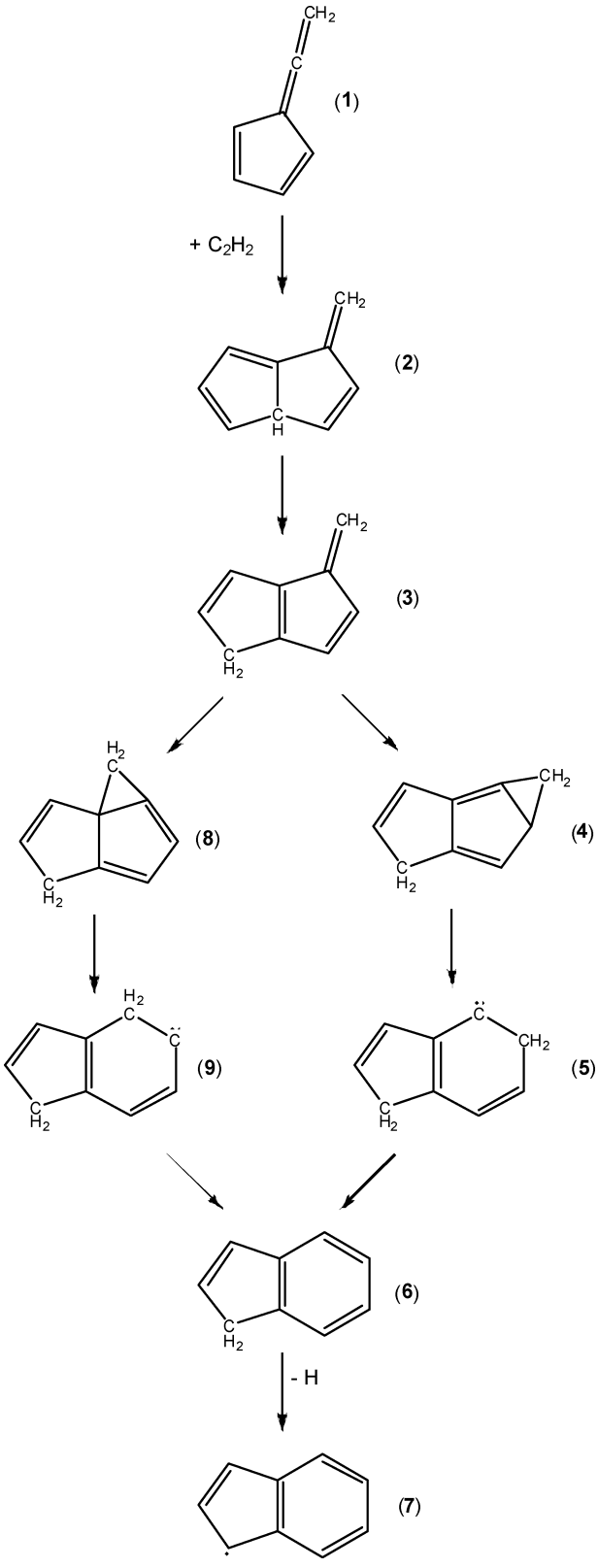

structure or van der Waals well. Rate constants have been calculated for structures at 0.1 Å intervals along the MEP in both the forward and reverse directions. Rate constants for the association reaction are plotted in Figure 2 as a function of temperature and position along the MEP (only the contributing transition state structures are included). From Figure 1 we see

TABLE 1: Standard Enthalpies of Formation ($\Delta_f H°_{298}$, kcal mol^{-1}) for Stable Molecules and Transition States in the Fulvenallene (1) + C_2H_2 Mechanism (Calculated at the G3B3 Level of Theory from Atomization Work Reactions)[a]

	$\Delta_f H°_{298}$ (kcal mol^{-1})
C_2H_2	54.6
fulvenallene (**1**)	85.3
2	83.3
3	77.3
4	117.8
5	127.0
indene (**6**)	39.8
1-indenyl (**7**)	68.6
8	120.4
9	128.4
TS1	166.6
TS2	106.6
TS3	118.7
TS4	138.6
TS5	127.0
TS7	120.2
TS8	140.6
TS9	129.0

[a] Molecule and transition state numbering is defined in Scheme 2 and Figure 6.

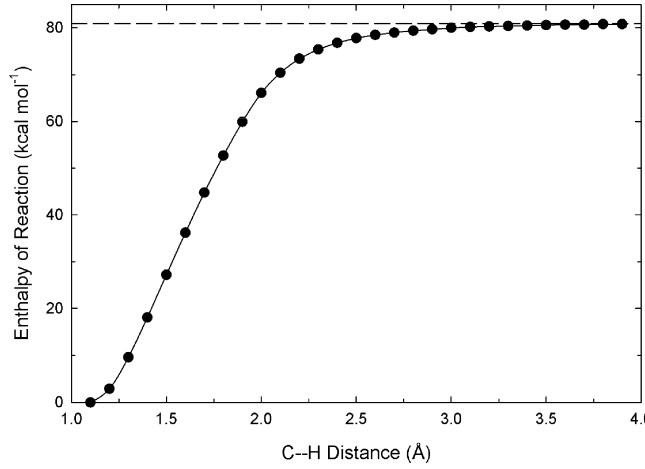

Figure 1. Minimum energy potential for C−H bond dissociation in indene (**6**). Calculated at the B3LYP/6-31G(d) level, scaled by the G3B3 298 K enthalpy of reaction (relative to indene (**6**)). Dashed line indicates energy of infinitely separated products.

that the association reaction demonstrates a small positive activation energy with rate constants between 3 and 7 × 10^{13} cm^3 mol^{-1} s^{-1}. The variational rate constant is provided by the 3.0 Å structure at 300 K, moving through several other structures with increasing temperature, and ultimately to a 2.3 Å transition state at 1800 K and above (see Figure 3). The minimum rate constant between 300 and 2000 K has been fit to a three-parameter Arrhenius equation. For the dissociation reaction we find k [s^{-1}] = 4.95 × $10^{14}T^{0.148}$ exp(−40780/T) and for the association reaction k [cm^3 mol^{-1} s^{-1}] = 8.20 × $10^{13}T^{-0.0107}$ exp(−232/T).

Relatively little prior work is available on the 1-indenyl + H reaction or on thermal decomposition of indene. Marinov et al.[9] assumed a temperature-independent rate constant of 2 × 10^{14} cm^3 mol^{-1} s^{-1} for the 1-indenyl + H → indene reaction, typical of H addition at an unsaturated carbon radical site. This rate constant has since been used in several other kinetic models for PAH formation.[5,36] At 300 K, our calculated rate constant is around a factor of 6 below the Marinov et al. estimate. This

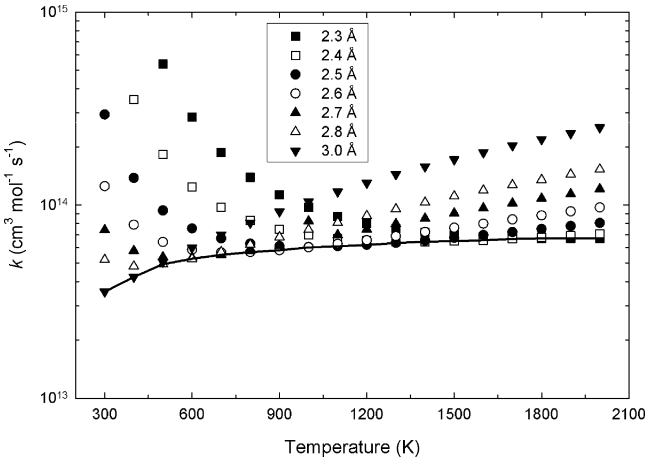

Figure 2. Rate constants for the 1-indenyl (**7**) + H association reaction, as a function of C−H bond length and temperature. Solid line indicates the minimum, or variational, rate constant.

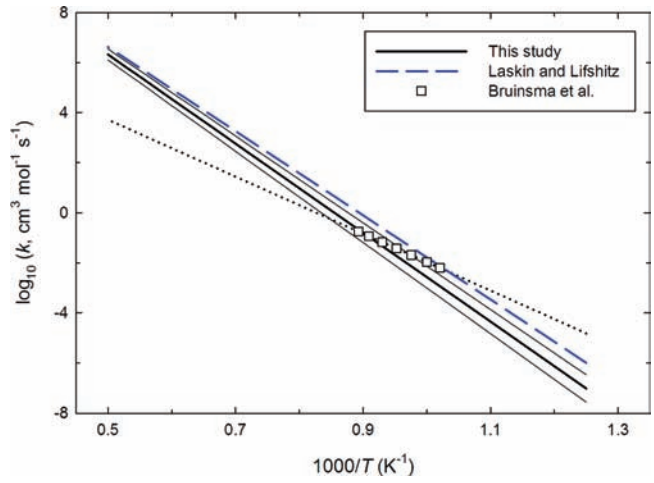

Figure 4. Rate constants for the thermal decomposition of indene (**6**) to 1-indenyl (**7**) + H. Results of this study are from canonical VTST calculations (faint lines indicate uncertainty in E_a of ±2 kcal mol^{-1}). Dotted line indicates extrapolation of the Bruinsma et al. experimental rate expression between 800 and 2000 K.

discrepancy decreases with increasing temperature, due to the small activation energy predicted here, and at 2000 K the two rate constants agree to within a factor of 3. Bruinsma et al.[39] experimentally studied the thermal decomposition of indene to unidentified products in the narrow temperature range 980−1120 K. They obtained the rate expression $k = 2.59 \times 10^9$ exp(−26220/T) s^{-1}, where the activation energy is 52.1 kcal mol^{-1}. Laskin and Lifshitz estimated the rate expression $k = 1.1 \times 10^{15}$ exp(−38800/T) s^{-1} for dissociation to indene to 1-indenyl + H;[40] their activation energy of 77 kcal mol^{-1} is in relatively close agreement with our calculated activation energy of 80.9 kcal mol^{-1}. Our calculated rate expression for decomposition of indene to 1-indenyl + H is plotted in Figure 4 along with the experimental results of Bruinsma et al.[39] (where their rate expression is extrapolated over 800−2000 K) and the estimated rate constants of Laskin and Lifshitz.[40] Our calculated rate constants are similar to those estimated by Laskin and Lifshitz,[40] agreeing to almost within the computational uncertainty. Furthermore, for the temperature range in which the experimental results were obtained there is actually relatively good agreement between the experimental and theoretical results despite the large difference in activation energy. At 1120 K, the experimental rate constant is 0.179 s^{-1}, whereas our rate expression provides a value of 0.22 s^{-1}. The results differ somewhat at lower temperatures, but even then the differences are close to the computational uncertainty. If the experimental rate expression is extrapolated over a wider temperature range, however, the experimental and theoretical results begin to diverge significantly. It is likely that Bruinsma et al.[39] were observing indene decomposition to 1-indenyl + H, although we are unable to state why their lower-temperature results could be in error (nor can we exclude the possibility of a lower-energy decomposition pathway to different products).

Transition States and Elementary Reaction Rates. Rate parameters E_a, A', and n for each of the elementary reaction processes are listed in Table 2, calculated from thermochemical properties of the reactants, products, and transition states. Transition state geometries for each of the reaction steps are relatively conventional, except perhaps for the acetylene + fulvenallene transition state (**TS1**, depicted in Figure 5). Acetylene addition occurs primarily at the allene carbon site (=C=), with a relatively product-like C−C bond length of 1.8 Å. Interaction of the terminal acetylene CH group with a ring carbon atom is weak, and formation of this bond occurs late along the association reaction coordinate (i.e., reactant-like). Intrinsic reaction coordinate (IRC) analysis was performed for **TS1** in both directions where further optimization of the forward and reverse IRC structures yielded the stated reactants and products.

Potential Energy Surface. Energy diagrams for the parallel reaction mechanisms proposed in Scheme 2 are depicted in Figure 6 (the energy diagrams feature G3B3 heats of formation).

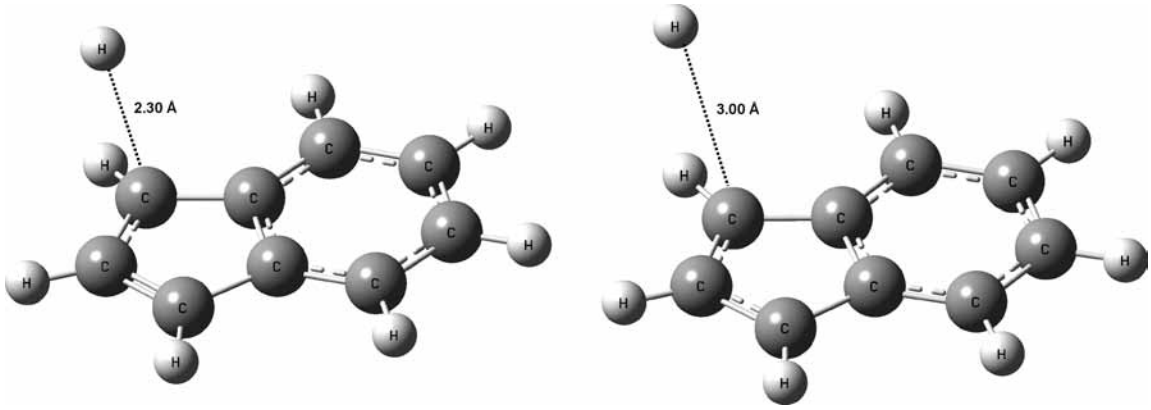

Figure 3. High- and low-temperature variational transition state structures for the 1-indenyl (**7**) + H association reaction at the B3LYP/6-31G(d) level.

TABLE 2: Elementary Rate Parameters (A', n, E_a) for Forward (f) and Reverse (r) Reactions in the Proposed Fulvenallene (1) + C_2H_2 Mechanism[a]

	A' (f)	n (f)	E_a (f)	A' (r)	n (r)	E_a (r)
fulvenallene (**1**) + C_2H_2 → **2** (**TS1**)	1.63×10^4	2.442	26.31	6.59×10^{11}	1.382	83.57
2 → **3** (**TS2**)	3.35×10^9	1.065	21.97	2.15×10^9	1.070	27.93
3 → **4** (**TS3**)	3.05×10^{12}	0.048	41.93	5.42×10^{12}	0.118	1.48
4 → **5** (**TS4**)	5.91×10^{12}	0.199	21.39	5.21×10^{12}	−0.016	12.25
5 → indene (**6**) (**TS5**)	3.35×10^{11}	0.310	0.24	9.99×10^{10}	0.839	87.22
Indene (**6**) → 1-indenyl (**7**) + H (**TS6**)	4.95×10^{14}	0.148	81.03	8.20×10^{13}	−0.011	0.46
3 → **8** (**TS7**)	2.44×10^{12}	0.070	43.43	5.17×10^{12}	0.032	0.39
8 → **9** (**TS8**)	8.44×10^{12}	0.046	20.81	4.02×10^{12}	−0.013	12.84
9 → indene (**6**) (**TS9**)	3.88×10^{11}	0.300	0.71	2.49×10^{11}	0.812	89.11

[a] $k = A'T^n \exp(-E_a/RT)$. Units: s, cm^3, mol, kcal mol^{-1}. Molecule and transition state numbering is defined in Scheme 2 and Figure 6.

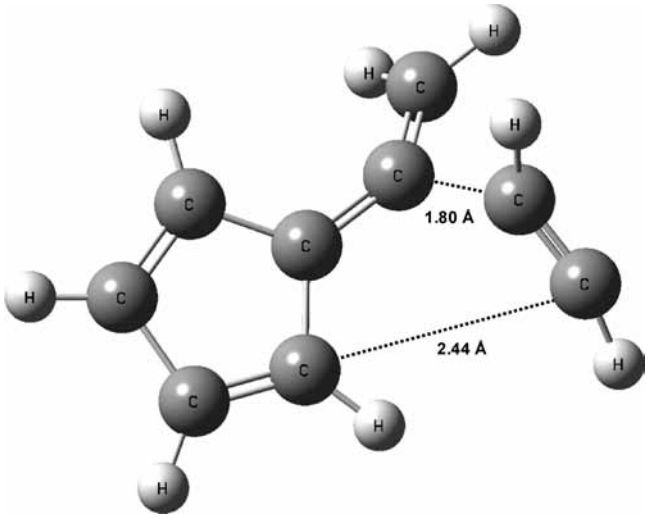

Figure 5. Transition state structure for acetylene addition to fulvenallene (**1**) at the B3LYP/6-31G(d) level.

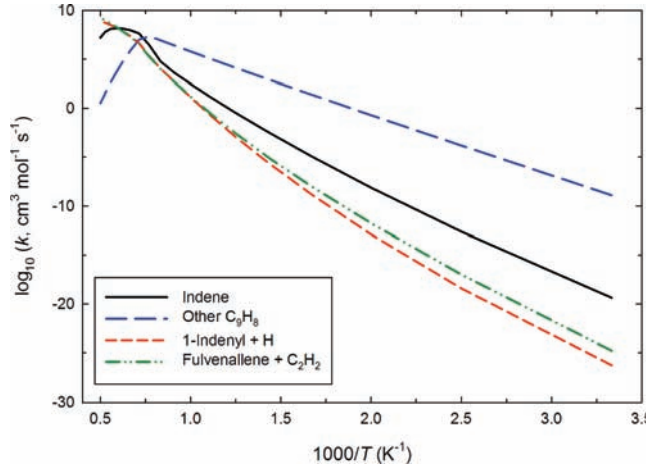

Figure 7. Rate constants in the chemically activated fulvenallene (**1**) + C_2H_2 reaction at 1 atm.

We find that acetylene adds to fulvenallene with a barrier of around 27 kcal mol^{-1}; while this is a significant barrier, it is relatively low for the association of two stable species. The association reaction produces an acetylene-fulvenallene adduct with ca. 80 kcal mol^{-1} of excess vibrational energy. The large well-depth for this reaction provides the adduct with significant energy to undergo the fulvene-benzene rearrangement, where the maximum barrier height is around 20 kcal mol^{-1} below the energy of the entrance channel. Indene lies about 100 kcal mol^{-1} below fulvenallene + acetylene, or nearly 130 kcal mol^{-1} below

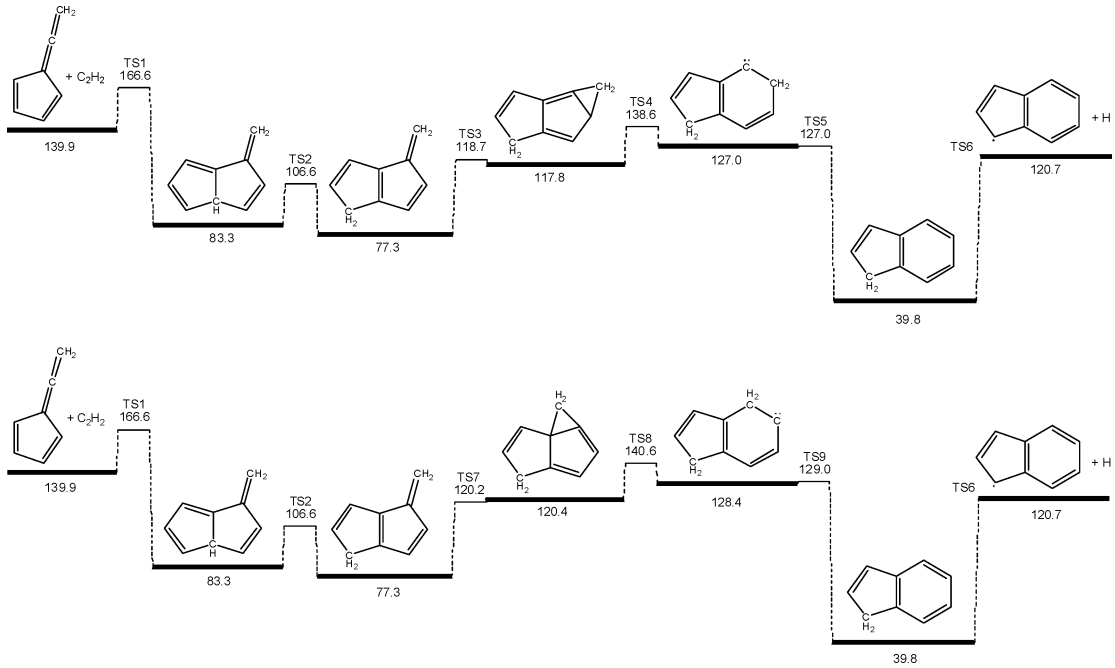

Figure 6. Energy diagrams for indene (**6**) and 1-indenyl (**7**) + H formation from reaction of fulvenallene (**1**) + acetylene (G3B3 $\Delta_f H°_{298}$, kcal mol^{-1}).

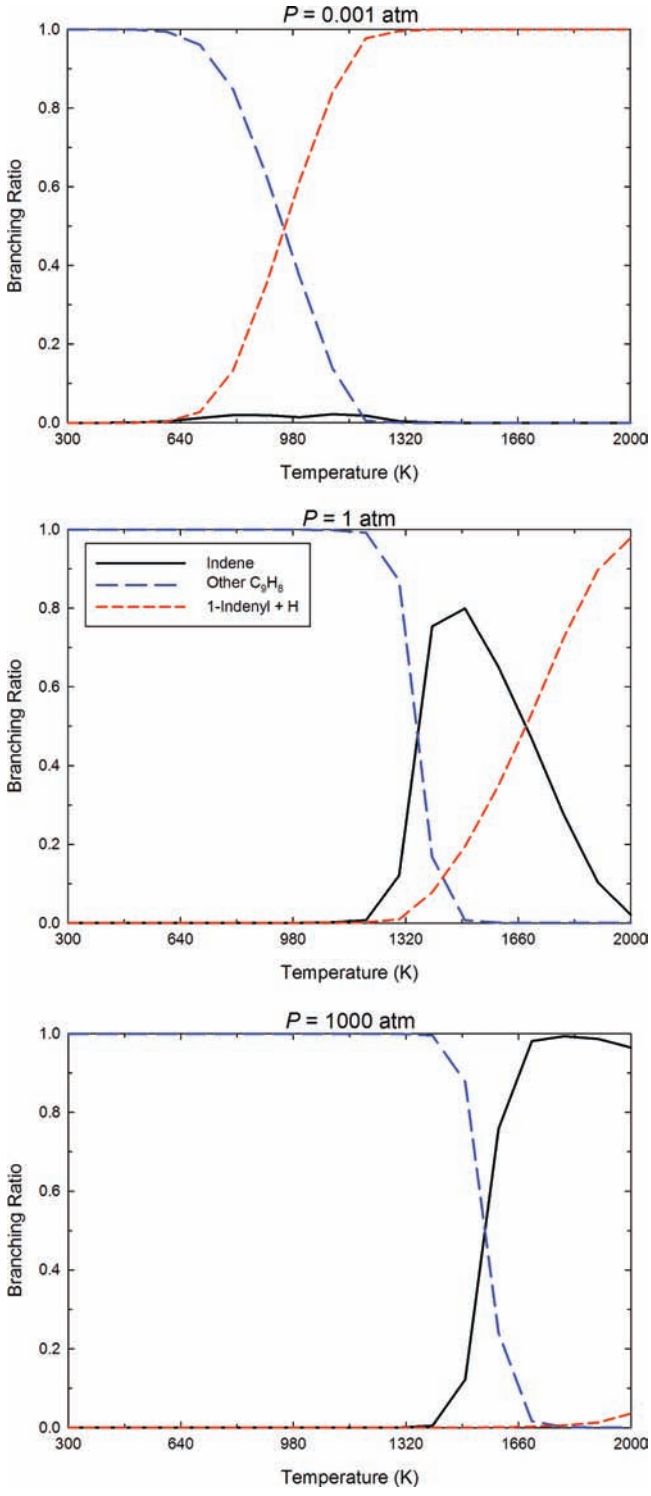

Figure 8. Branching ratios to C_9H_8 isomers in the chemically activated fulvenallene (**1**) + C_2H_2 reaction at varied pressures.

the association transition state energy, and dissociation of collision stabilized C_9H_8 molecules back to these reactants is not expected to be significant. Dissociation of indene to 1-indenyl + H requires ca. 80 kcal mol^{-1}, which is significantly below the energy of the reactants; accordingly, a significant fraction of the activated C_9H_8 adduct population should possess sufficient energy to proceed to 1-indenyl + H, depending on the temperature and pressure conditions. Of the two isomeric channels for conversion of **3** to **6**, the one proceeding via **TS4** is 2 kcal mol^{-1} lower in energy. This channel is expected to dominate the flux of **3** to **6** and back and is the only one considered below in our qRRK/ME calculations.

TABLE 3: Input Rate Parameters (A', n, E_a) for Modelling the Chemically Activated Fulvenallene (1) + C_2H_2 Reaction at 1 atm Pressure[a]

	A'	n	E_a
fulvenallene + C_2H_2 → cyclopentadiene-fulvene (**2** + **3**) [300−1300 K]	8.45×10^{4}	2.22	26.53
fulvenallene + C_2H_2 → cyclopentadiene-fulvene (**2** + **3**) [1300−2000 K]	3.99×10^{305}	−87.24	156.49
fulvenallene + C_2H_2 → indene [300−1600]	3.22×10^{-51}	19.42	23.23
fulvenallene + C_2H_2 → indene [1600−2000]	1.44×10^{292}	−78.17	245.01
fulvenallene + C_2H_2 → 1-indenyl + H	9.70×10^{-42}	16.72	37.52

[a] $k = A'T^n \exp(-E_a/RT)$. Units: s, cm^3, mol, kcal. Valid for the range 300−2000 K.

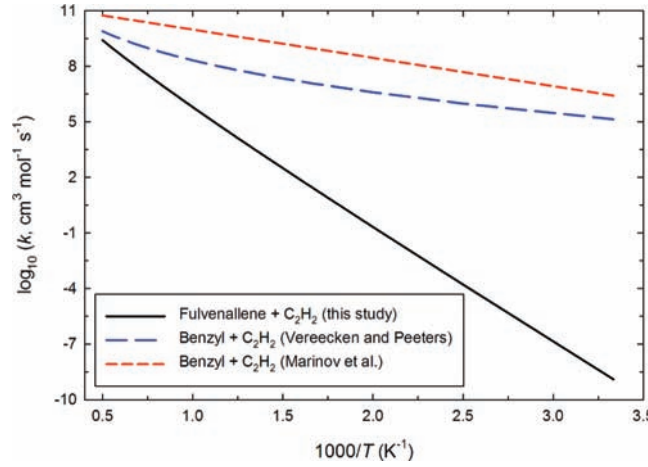

Figure 9. Comparison of rate expressions for the fulvenallene (**1**) + C_2H_2 and benzyl + C_2H_2 reactions to C_9 products.

Reaction Kinetics. The fulvenallene + C_2H_2 (+M) → indene (+M)/1-indenyl + H (+M) reaction has been simulated using qRRK/ME theory for temperature and pressure conditions of 300−2000 K and 0.001−1000 atm. In our analysis, we consider pathways to the products indene, 1-indenyl + H, fulvenallene + C_2H_2, and other C_9H_8 isomers. The fulvenallene + C_2H_2 product set represents the reverse dissociation reaction of the activated C_9H_8 adduct, and constitutes no net reaction. The lumped C_9H_8 isomers essentially comprise the cyclopentadiene-fulvene species **2** and **3**, as **4** and **5** are relatively unstable; the distribution of **2** and **3** is expected to approach equilibrium in any system of interest, given the small barrier for isomerization (<30 kcal mol^{-1}).

Rate constants to the three product channels and for the reverse reaction are plotted in Figure 7 for 1 atm pressure. Branching ratios for the forward reaction channels are depicted in Figure 8, along with results at 0.001 and 1000 atm. Formation of the stabilized C_9H_8 isomers **2** and **3** dominates at low temperatures, where there is insufficient energy for isomerization to indene or dissociation back to fulvenallene + C_2H_2. For atmospheric pressure, formation of indene becomes the dominant process at around 1300 K. As the temperature increases to around 1700 K there is sufficient energy for dissociation to 1-indenyl + H (80.9 kcal mol^{-1} above indene) and to fulvenallene + C_2H_2 (83.3 kcal mol^{-1} above the initial fulvenallene-acetylene adduct). At lower pressures, where collision stabili-

zation is less important, quenching of indene is not significant. At low temperatures, the major products are the other C_9H_8 isomers, with 1-indenyl + H being important at higher temperatures. This result implies that the fraction of the activated adduct population that transforms to indene has sufficient energy to dissociate to 1-indenyl + H before collision stabilization. At higher pressures we find that the formation of 1-indenyl + H becomes a relatively unimportant process; at lower temperatures the major products are the other C_9H_8 isomers, while for higher temperatures isomerization to indene followed by collision stabilization dominates.

Fitted rate parameters for the formation of new product sets in the chemically activated fulvenallene + C_2H_2 reaction are provided in Table 3 for use in kinetic models. Rate parameters are at 1 atm pressure with results at other pressures available in the Supporting Information. The reactions producing quenched C_9H_8 isomers (indene and the other C_9H_8 species) demonstrate complex kinetics with rate constants both increasing and decreasing with increasing temperature. This data required separate fits across low-temperature and high-temperature regimes. Alternatively, the total forward reaction rate to all C_9H_8 isomers plus the 1-indenyl radical + H is described by the rate expression $k = 4.62 \times 10^{13} T^{-0.438} \exp(-15010/T)$ cm^3 mol^{-1} s^{-1}, where the product distribution is given by the branching ratios in Figure 8. This overall forward reaction rate is relatively insensitive to pressure and provides a more straightforward means for including the fulvenallene + C_2H_2 process in kinetic models, given inclusion of accurate rate expressions for the indene ↔ 1-indenyl + H reactions.

In the activation reaction of fulvenallene with acetylene, this study considers the significant products to be indene, the cyclopentadiene-fulvene C_9H_8 isomers (**2** and **3**), and the 1-indenyl radical + H. Following collision stabilization, **1** and **2** will rearrange to indene, and potentially dissociate to 1-indenyl + H, with an activation energy of around 60 kcal mol^{-1}. The dissociation reaction back to fulvenallene + C_2H_2 is unlikely to be important because of the high barrier (83.3 kcal mol^{-1}). Indene produced in this mechanism, and by other pathways, is relatively stable toward the reactions considered here, and should be available to participate in bimolecular reactions, including PAH growth processes. At higher temperatures, indene will dissociate to 1-indenyl + H with activation energy of around 80 kcal mol^{-1}, and this reaction will dominate over isomerization back to the other C_9H_8 isomers. The indenyl radical formed in this reaction will participate in molecular weight growth reactions.

Role in PAH Formation. Kinetic modeling of PAH formation indicates that the benzyl + C_2H_2 reaction is an important contributor to the formation of C_9 aromatics.[10] The benzyl + C_2H_2 addition reaction proceeds with a barrier of 12 to 13 kcal mol^{-1},[8,11] significantly lower than that for the fulvenallene + C_2H_2 reaction. However, in the benzyl + C_2H_2 mechanism there is significant reverse dissociation of the C_9H_9* adduct, decreasing the forward reaction rate to C_9 species at high temperatures and low pressures.[11] At 1 atm, Vereecken and Peeters[11] calculated the rate expression $k = 3.12 \times 10^{-6} T^{4.712} \exp(-12500/T)$ cm^3 mol^{-1} s^{-1} for the benzyl + acetylene reaction, whereas Marinov et al.[9] had previously estimated $k = 3.2 \times 10^{11} \exp(-3520/T)$ cm^3 mol^{-1} s^{-1} for the same reaction. These two rate expressions are plotted in Figure 9, compared to the total rate constant for C_9 species formation in the fulvenallene + C_2H_2 reaction ($k = 4.62 \times 10^{13} T^{-0.438} \exp(-15010/T)$ cm^3 mol^{-1} s^{-1}). The Marinov et al. benzyl + C_2H_2 rate constants are considerably greater than those calculated by Vereecken and Peeters, but both come into relative agreement if an activation energy of 12−13 kcal mol^{-1} is used in the Marinov et al. rate expression. Because of the considerably greater barrier for C_2H_2 addition to fulvenallene than to benzyl, these rate constants are several orders of magnitude smaller at low temperatures. At higher temperatures, however, the rate constant for the fulvenallene + C_2H_2 reaction approaches that of benzyl + C_2H_2 (based on the Vereecken and Peeters results), being less than a factor of 5 slower at 1800 K and above. This is due to the increased importance of entropy at higher temperatures, as well as the significant reverse reaction taking place in the benzyl mechanism above around 1000 K.

As the fulvenallene + C_2H_2 reaction proceeds at a rate approaching that of the benzyl + C_2H_2 reaction at combustion temperatures, the importance of this new mechanism will depend largely on the relative concentrations of benzyl and fulvenallene. Both benzyl and fulvenallene have been detected at high concentrations in a fuel-rich toluene/O_2 flame, with respective peak mole fractions of 1.2×10^{-3} and 6.3×10^{-4}.[22] Under these conditions, the benzyl + C_2H_2 contribution to C_9 species formation is predicted to be around 10 times as important as the fulvenallene + C_2H_2 reaction at 1800 K. Benzyl is present at highly elevated levels in toluene flames due to the very weak $C_6H_5CH_2$—H bond in toluene, and the fulvenallene + C_2H_2 mechanism may play a greater role in other combustion systems, where it is not formed via benzyl decomposition. For example, fulvenallene is expected to form via low-energy processes in the C_5H_5 + C_2H_2 reaction. In a cyclopentane flame, a C_7H_6 species thought to be fulvenallene has been detected at peak mole fractions of ca. 5×10^{-5}, around five times the peak concentration of C_7H_7 species (likely benzyl + cycloheptatrienyl).[23] When the fulvenallene concentration is five times that of benzyl, we predict that the fulvenallene + C_2H_2 reaction is more important in C_9 aromatic formation than benzyl + C_2H_2 for temperatures of around 1800 K and above. While further work is required to characterize fulvenallene concentrations in different combustion systems, it is apparent from the present analysis that the fulvenallene + C_2H_2 reaction will be of at least some importance to indene formation in C_5 and C_6 flames.

Conclusions

Thermochemical data and kinetics are provided for the fulvenallene + C_2H_2 reaction system. Fulvenallene is a recently identified combustion intermediate not presently considered in kinetic models and is expected to play a role in the formation of PAHs and soot. Fulvenallene associates with C_2H_2 with a barrier of around 26 kcal mol^{-1}, forming an activated cyclopentadiene-fulvene type adduct. This adduct can rearrange to indene, then dissociate to 1-indenyl + H, with barriers below the entrance channel energy. qRRK/ME simulations reveal that indene and 1-indenyl + H are the dominant products at higher temperatures, while stabilized cyclopentadiene-fulvene radicals form at lower temperatures. Improved rate constants are also provided for the 1-indenyl + H association reaction, and the reverse dissociation, from variational transition state theory.

Acknowledgment. J.W.B. acknowledges partial funding from ExxonMobil Scholarship and Research awards to the New Jersey Institute of Technology (Walt Weissman and John Farrell coordinators).

Supporting Information Available: Optimized geometries (in Cartesian coordinates); vibrational frequencies; G3B3 enthalpies (in hartrees); entropies and heat capacities; input rate

parameters for kinetic modeling at 0.001−1000 atm. This material is available free of charge via the Internet at http://pubs.acs.org.

References and Notes

(1) For example, see (a) Haynes, B. S.; Wagner, H. G. *Prog. Energy Combust. Sci.* **1981**, *7*, 229. (b) Kennedy, I. M. *Prog. Energy Combust. Sci.* **1997**, *23*, 95. (c) Richter, H.; Howard, J. B. *Prog. Energy Combust. Sci.* **2000**, *26*, 565. (d) Frenklach, M. *Phys. Chem. Chem. Phys.* **2002**, *4*, 2028.

(2) Durant, J. L.; Busby, W. F.; Lafleur, A. L.; Penman, B. W.; Crespi, C. L. *Mutat. Res.* **1996**, *371*, 123.

(3) Allen, J. O.; Dookeran, N. M.; Smith, K. A.; Sarofim, A. F.; Taghizadeh, K.; Lafleur, A. L. *Environ. Sci. Technol.* **1996**, *30*, 1023.

(4) Dockery, D. W.; Pope, C. A.; Xu, X.; Spengler, J. D.; Ware, J. H.; Fay, M. E.; Ferris, B. G.; Speizer, F. E. *New Engl. J. Med.* **1993**, *329*, 1753.

(5) Richter, H.; Grieco, W. J.; Howard, J. B. *Combust. Flame* **1999**, *119*, 1.

(6) Lu, M.; Mulholland, J. A. *Chemosphere* **2001**, *42*, 625.

(7) Kerner, R.; Penson, K. A.; Bennemann, K. H. *Europhys. Lett.* **1992**, *19*, 363.

(8) Kislov, V. V.; Mebel, A. M. *J. Phys. Chem. A* **2007**, *111*, 3922.

(9) Marinov, N. M.; Pitz, W. J.; Westbrook, C. K.; Castaldi, M. J.; Senkan, S. M. *Combust. Sci. Technol.* **1996**, *116*, 211.

(10) Sivaramakrishnan, R.; Tranter, R. S.; Brezinsky, K. *J. Phys. Chem. A* **2006**, *110*, 9400.

(11) Vereecken, L.; Peeters, J. *Phys. Chem. Chem. Phys.* **2003**, *5*, 2807.

(12) Granata, S.; Faravalli, T.; Ranzi, E.; Olten, N.; Senkan, S. *Combust. Flame* **2002**, *131*, 273.

(13) Kinetics for this reaction are estimated in ref 9 (reaction number 520) and used in numerous subsequent models; k [cm^3 mol^{-1} s^{-1}] = 3.20 × 10^{11} exp(−3520/T).

(14) (a) Brezinsky, K.; Litzinger, T. A.; Glassman, I. *Int. J. Chem. Kinet.* **1984**, *16*, 1053. (b) Bartels, M.; Edelbuttel-Einhaus, J.; Hoyermann, K. *Proc. Combust. Inst.* **1989**, *22*, 1041. (c) Hippler, H.; Reihs, C.; Troe, J. *Proc. Combust. Inst.* **1990**, *23*, 37. (d) Hoyerman, K.; Seeba, J.; Olzmann, M.; Viskolcz, B. *Ber. Bunsen-Ges. Phys. Chem.* **1997**, *101*, 538. (e) da Silva, G.; Bozzelli, J. W. *Proc. Combust. Inst.* **2009**, *32*, 287.

(15) (a) Nelson, H. H.; McDonald, J. R. *J. Phys. Chem.* **1982**, *86*, 1242. (b) Murakami, Y.; Oguchi, T.; Hashimoto, K.; Nosaka, Y. *J. Phys. Chem. A* **2007**, *111*, 13200.

(16) (a) Baulch, D. L.; Cobos, C. J.; Cox, R. A.; Esser, C.; Frank, P.; Just, T.; Kerr, J. A.; Pilling, M. J.; Troe, J.; Walker, R. W.; Warnatz, J. *J. Phys. Chem. Ref. Data* **1992**, *21*, 411. (b) Oehlschlaeger, M. A.; Davidson, D. F.; Hanson, R. K. *J. Phys. Chem. A* **2006**, *110*, 6649.

(17) (a) Fröchtenicht, R.; Hippler, H.; Troe, J.; Toennies, J. P. *J. Photochem. Photobiol., A* **1994**, *80*, 33. (b) Eng, R. A.; Gebert, A.; Goos, E.; Hippler, H.; Kachiani, C. *Phys. Chem. Chem. Phys.* **2002**, *4*, 3989.

(18) da Silva, G.; Cole, J. A.; Bozzelli, J. W. *J. Phys. Chem. A.* **2009**, *113*, 6111.

(19) Cavallotti, C.; Derudi, M.; Rota, R. *Proc. Combust. Inst.* **2009**, *32*, 115.

(20) Jones, J.; Bacskay, G. B.; Mackie, J. C. *J. Phys. Chem. A* **1997**, *101*, 7105.

(21) Wong, M. W.; Wentrup, C. *J. Org. Chem.* **1996**, *61*, 7022.

(22) Li, Y.; Zhang, L.; Tian, Z.; Yuan, T.; Wang, J.; Yang, B.; Qi, F. *Energy Fuels* **2009**, *23*, 1473–1485.

(23) Hansen, N.; Kasper, T.; Klippenstein, S. J.; Westmoreland, P. R.; Law, M. E.; Taatjes, C. A.; Kohse-Höinghaus, K.; Wang, J.; Cool, T. A. *J. Phys. Chem. A* **2007**, *111*, 4081.

(24) Baboul, A. G.; Curtiss, L. A.; Redfern, P. C.; Raghavachari, K. *J. Chem. Phys.* **1999**, *110*, 7650.

(25) Frisch, M. J.; Trucks, G. W.; Schlegel, H. B.; Scuseria, G. E.; Robb, M. A.; Cheeseman, J. R.; Montgomery, Jr., J. A.; Vreven, T.; Kudin, K. N.; Burant, J. C.; Millam, J. M.; Iyengar, S. S.; Tomasi, J.; Barone, V.; Mennucci, B.; Cossi, M.; Scalmani, G.; Rega, N.; Petersson, G. A.; Nakatsuji, H.; Hada, M.; Ehara, M.; Toyota, K.; Fukuda, R.; Hasegawa, J.; Ishida, M.; Nakajima, T.; Honda, Y.; Kitao, O.; Nakai, H.; Klene, M.; Li, X.; Knox, J. E.; Hratchian, H. P.; Cross, J. B.; Adamo, C.; Jaramillo, J.; Gomperts, R.; Stratmann, R. E.; Yazyev, O.; Austin, A. J.; Cammi, R.; Pomelli, C.; Ochterski, J. W.; Ayala, P. Y.; Morokuma, K.; Voth, G. A.; Salvador, P.; Dannenberg, J. J.; Zakrzewski, V. G.; Dapprich, S.; Daniels, A. D.; Strain, M. C.; Farkas, O.; Malick, D. K.; Rabuck, A. D.; Raghavachari, K.; Foresman, J. B.; Ortiz, J. V.; Cui, Q.; Baboul, A. G.; Clifford, S.; Cioslowski, J.; Stefanov, B. B.; Liu, G.; Liashenko, A.; Piskorz, P.; Komaromi, I.; Martin, R. L.; Fox, D. J.; Keith, T.; Al-Laham, M. A.; Peng, C. Y.; Nanayakkara, A.; Challacombe, M.; Gill, P. M. W.; Johnson, B.; Chen, W.; Wong, M. W.; Gonzalez, C.; Pople, J. A. *Gaussian 03*, rev. D.01; Gaussian, Inc.: Wallingford, CT, 2004.

(26) Eckart, C. *Phys. Rev.* **1930**, *35*, 1303.

(27) (a) da Silva, G. *Chem. Phys. Lett.* **2009**, *474*, 13. (b) da Silva, G.; Bozzelli, J. W.; Asatryan, R. *J. Phys. Chem. A*, DOI: 10.1021/jp904156r.

(28) Mokrushin, V.; Bedanov, V.; Tsang, W.; Zachariah, M.; Knyazev, V. *ChemRate*, Version 1.5.2; National Institute of Standards and Testing: Gaithersburg, MD, 2006.

(29) Chang, A. Y.; Bozzelli, J. W.; Dean, A. M. *Z. Phys. Chem.* **2000**, *214*, 1533.

(30) Sheng, C. Y.; Bozzelli, J. W.; Dean, A. M.; Chang, A. Y. *J. Phys. Chem. A* **2002**, *106*, 7276.

(31) Bozzelli, J. W.; Chang, A. Y.; Dean, A. M. *Int. J. Chem. Kinet.* **1997**, *29*, 161.

(32) (a) Madden, L. K.; Mebel, A. M.; Lin, M. C. *J. Phys. Org. Chem.* **1996**, *9*, 801. (b) Bettinger, H. F.; Schreiner, P. R.; Schaefer, H. F., III; Schleyer, P. V. R. *J. Am. Chem. Soc.* **1998**, *120*, 5741.

(33) Chase, M. W., Jr. *J. Phys. Chem. Ref. Data* **1998**, *9*, 1.

(34) Cox, J. D.; Pilcher, G. *Thermochemistry of Organic and Organometallic Compounds*; Academic Press: New York, 1985.

(35) Stein, S. E.; Brown, R. L. *J. Am. Chem. Soc.* **1991**, *113*, 787.

(36) Richter, H.; Benish, T. G.; Mazyar, O. A.; Green, W. H.; Howard, J. B. *Proc. Combust. Inst.* **2000**, *28*, 2609.

(37) da Silva, G.; Bozzelli, J. W. *J. Phys. Chem. A* **2008**, *112*, 3566.

(38) da Silva, G.; Liang, L.; Bozzelli, J. W.; Farrell, J. T. *J. Phys. Chem. A*, in press.

(39) Bruinsma, O. S. L.; Tromp, P. J. J.; de Sauvage Nolting, H. J. J.; Moulijn, J. A. *Fuel* **1988**, *67*, 334.

(40) Laskin, A.; Lifshitz, A. *Symp. (Int.) Combust.* **1998**, *27*, 313.

JP904261E